

# Out-of-plane actuation of silicon micro-cantilever based on (Pb, La) (Zr, Ti)O<sub>3</sub> antiferroelectric thick films

Jun Liu<sup>1</sup> · Kun An<sup>2</sup> · Li Liu<sup>3</sup> · Jian He<sup>1</sup> · Xiujuan Chou<sup>2</sup> · Chenyang Xue<sup>3</sup>

Received: 25 July 2015 / Accepted: 22 October 2015 / Published online: 31 October 2015  
© Springer Science+Business Media New York 2015

**Abstract** With micro-machining technologies, the micro-cantilevers of Si-based antiferroelectric (Pb, La) (Zr, Ti)O<sub>3</sub> thick films were fabricated, and five sizes of cantilevers were completed in one chip. Out-of-plane motion of the cantilever structure was described with the out-of-plane actuation method. Under the square wave excited by the voltage of  $42 \pm 2$  V, the micro-cantilevers presented the good performance, such as high vibration velocity of 0.93 m/s and big cantilever tip displacement of 31  $\mu$ m due to the electrical field induced phase transition in the thick film. The drive voltage as the phase-transition voltage was applied to the antiferroelectric material layers for the out-of-plane motions measured by Micro System Analyzer (MSA-400), and hence the 1st-order resonance frequency of the cantilevers was 40.08 kHz. These results reveal that the antiferroelectric thick films (Pb, La) (Zr, Ti)O<sub>3</sub> are of characteristics of large electrostrictive strain and show the potential and board application for the micro-devices with those films in micro-actuators and high-speed digital switches.

## 1 Introduction

The antiferroelectric (AFE) material have a unique phase transition characteristic between the AFE phase and the ferroelectric (FE) phase, characterized by remarkable change of polarization, phase-transition strain and phase-transition current under the field of electricity, pressure or temperature [1, 2]. When the AFE material changes from AFE phase to FE phase, the volume will become larger due to the larger unit cells. It was reported that the AFE material strain of (Pb, La) (Zr, Ti, Sn)O<sub>3</sub> was up to 0.85 % and the switching time of phase transition was about 300 ns [3–6]. Because of the unique phase transition effect and the large strain characteristic, the AFE material can take extensive application in micro-displacement actuators, force-electric coupling devices and micro-motors [7–9], etc. Compared to AFE ceramics bulk and AFE thin films, AFE thick films have lower transition voltage, more homogeneous and larger strain. To the best of our knowledge, it is rarely reported to integrate AFE thick films with MEMS techniques together to meet the demands in high-power micro-actuators.

In our earlier work, PLZT thick films has been successfully prepared on Pt(111)/Ti/SiO<sub>2</sub>/Si(100) substrate [10–12]. In this paper, the micro-cantilever structure based on the PLZT thick film was taken as the drive unit to apply AFE thick films in the field of MEMS. And the performance of cantilevers has been studied, including resonance frequencies, vibration modes, phased transition voltages of the AFE material layers and the switch strain, through the out-of-plane motions measured by the Micro System Analyzer, MSA-400.

---

✉ Xiujuan Chou  
chouxujuan@nuc.edu.cn

<sup>1</sup> Key Laboratory of Instrumentation Science and Dynamic Measurement, North University of China, Ministry of Education, Taiyuan, China

<sup>2</sup> National Key Laboratory for Electronic Measurement Technology, Taiyuan, China

<sup>3</sup> School of Instrument and Electronics, North University of China, Taiyuan, China

## 2 Design, fabrication and packaging

The fabrication of PLZT thick films and micro-cantilevers structure can be found elsewhere [13–16]. The device structure of micro-cantilevers can be obtained by the wet etching of AFE thick films and ICP dry etching of Silicon substrate. The complete structural layout of the AFE PLZT micro-cantilever was illustrated in Fig. 1. This layout was designed on a c-Si wafer with 3-in. diameter and 235- $\mu\text{m}$  thickness. The etching depth was 228  $\mu\text{m}$ , considering about 7  $\mu\text{m}$  thickness of silicon substrate in micro-cantilevers. A corrosion window of  $1360 \times 1360 \mu\text{m}^2$  was opened on the backside of the wafer. The thickness of AFE PLZT film was 2  $\mu\text{m}$ . The bottom electrode windows were arranged as ten cantilever beams and each beam had an independent bottom electrode. The pad area was  $100 \times 100 \mu\text{m}^2$ . The square shape was double-side aligned marker for wet etching and the cross shape was aligned marker for other layers. The name and function of layout were shown in Table 1 in detail. Figure 2 showed the SEM images of AFE PLZT micro-cantilevers. The SEM images of the device structure with ten cantilevers in five couple different sizes were shown in Fig. 2). All values for PLZT micro-cantilevers dimensions were listed in Table 2. The AFE PLZT micro-cantilevers that consist of polysilicon and PLZT multi-layer coating were shown in Fig. 2b.

The Fig. 3a showed the entire layout of two wafers integrated into one Printed Circuit Board (PCB) packaging. The cantilevers electrode was connected with PCB by Au bond wired (marked in red color). The bottom electrodes on one side were the same as those of the other side. From

Fig. 3b, the case package volume of the AFE PLZT micro-cantilevers was  $9 \times 9 \times 3 \text{ mm}^3$ .

## 3 Test and analyses

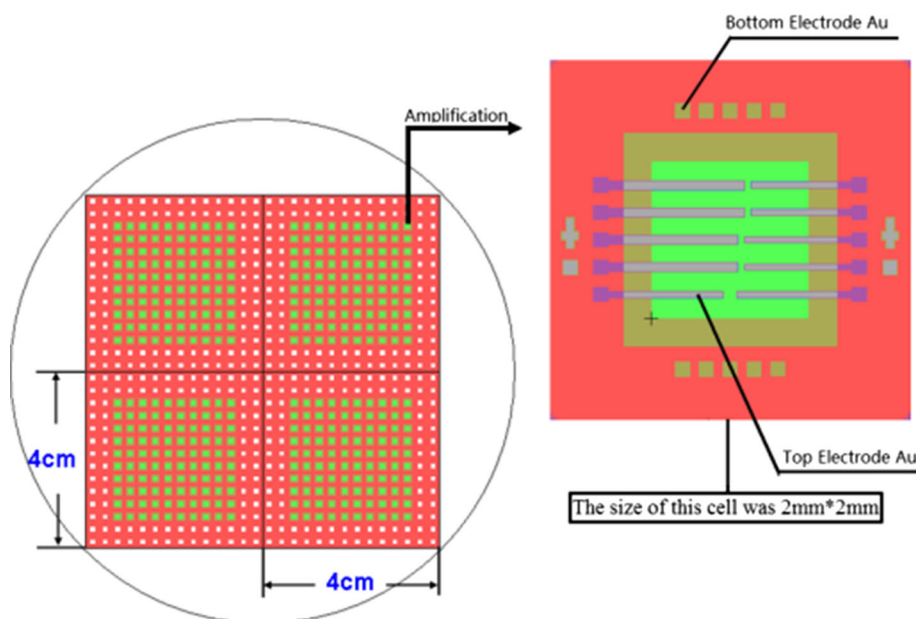
In order to obtain the electromechanical response behaviors (including resonant frequency, vibration velocity, and tip deflection) of the PLZT micro-cantilevers, Out-of-plane motions measured by Micro System Analyzer (MSA-400) was used with the laser Doppler method, which increased the flexibility and precision of non-contact measurement. The measurement processes were listed as followed.

Firstly, the signal generator of the micro-system analyzer offered a variety of signal modes (e.g., sweep, square wave and sine signals, etc.). Secondly, the maximal amplitude of original signal was amplified by the power

**Table 1** Revision illustrate of PLZT micro-cantilever in procedures

Photolithography order	Version number	Functions	Version class
1	Align	Alignment mark of dual surface Lithography	Negative version
2	Beam	Lithography in the cantilever beam	Positive version
3	Upper electrode	Lithography in the upper electrode	Positive version
4	Bottom electrode	lithography in the bottom electrode	Positive version

**Fig. 1** Complete structural layout of anti-ferroelectric PLZT micro-cantilever



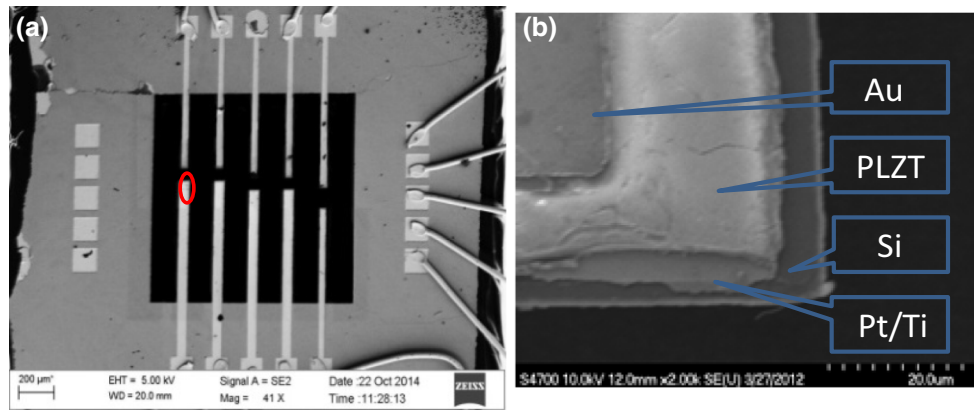


**Fig. 2** SEM images of antiferroelectric PLZT micro-cantilevers. **a** One device structure with ten cantilevers in five different sizes; **b** SEM image of cantilever tip

**Table 2** PLZT micro-cantilever dimensions

Samples	Length $l$ ( $\mu\text{m}$ )	Width $w$ ( $\mu\text{m}$ )	Thickness $t$ ( $\mu\text{m}$ )
Sample A	400	40	10
Sample B	450	40	10
Sample C	500	40	10
Sample D	600	60	10
Sample E	650	60	10

amplifier (HA-400) to 400 V-pp, to meet the requirement of phase transition voltage for the AFE thick film layer of the cantilevers. Finally, the magnified voltage was loaded into the cantilever while the oscilloscope and millimeters were adopted to inspect the loaded signals. The operating scheme of the system was showed in Fig. 4. The motion of the AFE PLZT micro-cantilevers was characterized by the Laser Doppler Vibrometer when applying the amplified sweep or sine/square voltages to the top and bottom electrodes. These measurements were performed at ambient temperature and pressure. The length ( $l$ ), width ( $b$ ) and thickness ( $t$ ) of the test cantilevers chosen as the sample were 500, 40 and 10  $\mu\text{m}$ , respectively. And 25 linear test points were set from top (the 1st) to bottom (the 25th) of the cantilever. All the test data were achieved by the setting

points of the certain size to indicate the vibration characteristics.

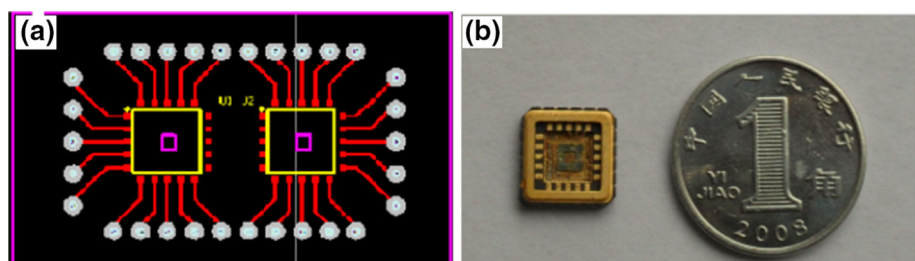
The thickness ( $t$ ) and the phase switching electric field ( $E$ ) of AFE PLZT films were about 2  $\mu\text{m}$  and 210 kV/cm, respectively. According to the formula of  $U = E \times t$ , the theoretical driving voltage was  $U = 210 \times 2 = 42$  V.

However, the maximal output voltage provided by POLYTEC System was only 10 V, and then an external power amplifier was required to amplify the voltage more than the phase transition voltage. Figure 5 was the simple test with Laser Doppler Vibrometer, and the inset showed the colorful photomicrograph and the photograph of AFE PLZT micro-cantilevers under microscope.

The resonance frequencies and the vibration modes were obtained by the sweep frequency test. The main setting parameters included Fast Fourier Transform (FFT) measurement modes, periodic chirp wave form, bandwidth of 0–500 kHz, the FFT algorithm with line 6400 (maximum), voltage amplitude of 1 V, and offset of 1 V.

The inset of Fig. 6 gave the sweep frequency signal of cantilever under the bias voltage of 10 V. The large strain magnitude of the cantilever was tested, and thus the phase transition characteristics were determined, including the AFE material layers with the response measurement of the vibration velocity and the displacement. The square signal with the step voltage magnitudes from 5, 7.5 to 60 V was

**Fig. 3** Package of antiferroelectric PLZT micro-cantilevers. **a** Layout of PCB packaging; **b** photograph of case package (Color figure online)



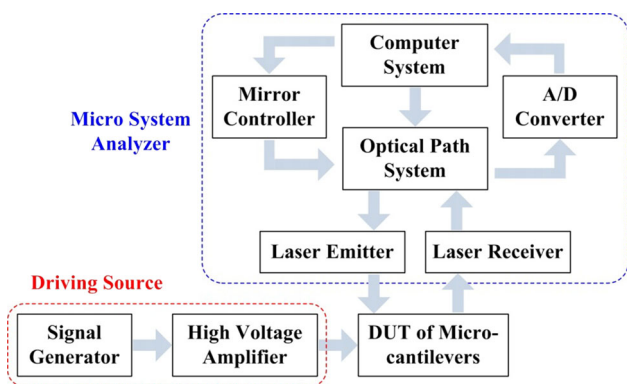


**Fig. 4** Measurement system of Micro System Analyzer and high voltage amplifier

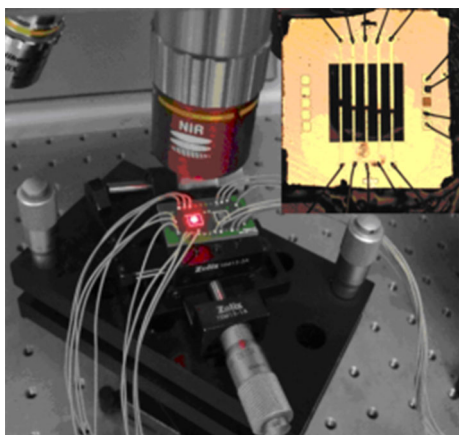
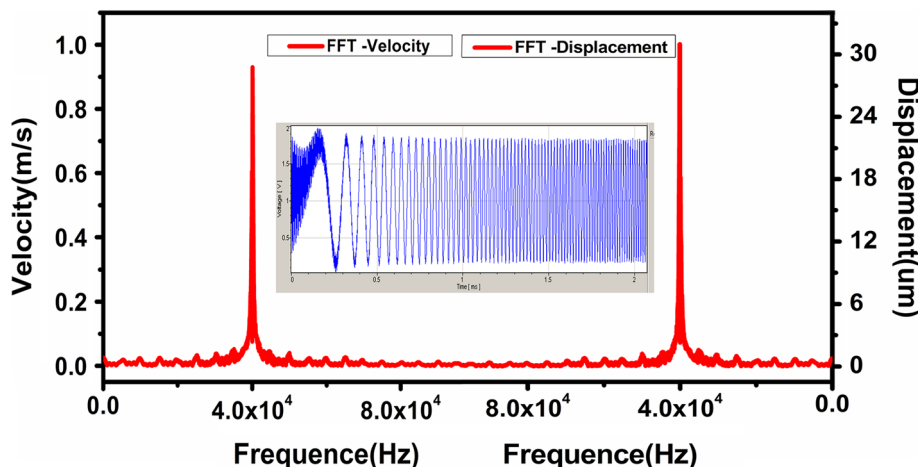


**Fig. 5** Simple test of Laser Doppler Vibrometer. The inset showed both the colorful photomicrograph and the antiferroelectric PLZT micro-cantilevers under microscope

loaded in the cantilevers, and the vibration velocity and displacement magnitudes were shown in Fig. 6.

Figure 6 showed the test result of frequency domain analysis (FFT) of the cantilevers tip (the 1st test point) at

**Fig. 6** Vibration velocity and displacement of the cantilever tip ( $500 \times 40 \times 10 \mu\text{m}^3$ ) with frequency domain analysis of FFT. The inset showed the period sweep frequency signal of Micro System Analyzer and the signal generator



the 15 V periodic chirp scan signal. There were one resonance peak of  $31 \mu\text{m}$  close to  $40.08 \text{ kHz}$ , and one vibration velocity about  $0.93 \text{ m/s}$ . Both the maximal vibration displacement and the vibration velocity were located near the first response frequency peak. And Fig. 7 showed the 1st-order vibration effect simulation at the first response of the cantilevers.

Figure 8 showed the curve relating the dependence of both maximal velocity and maximal displacement variation under different voltages of micro-cantilevers. The square voltage signals from  $-1$  to  $1 \text{ V}$  were applied to AFE PLZT micro-cantilevers, which was shown in the inset of Fig. 8. If the range was from  $a$  to  $b \text{ V}$ , the bias voltage (denoted as  $B$ ) and the voltage amplitude (denoted as  $A$ ) were expressed as follows,

$$B = \frac{a + b}{2} \tag{1}$$

$$A = \frac{b - a}{2} \tag{2}$$

From Eqs. (1), (2) and Fig. 8, the bias voltage ( $B$ ) was  $0 \text{ V}$  and the amplitude of voltage ( $A$ ) was  $1 \text{ V}$ . The cantilevers tip deflection tests were performed with square signal of the power amplifier that could be amplified from  $5, 7.5$  to  $75 \text{ V}$ . The maximum displacement and rate of the micro-cantilevers varied linearly with voltage in Fig. 8. There were three states to explain the phenomenon above. The first one was the quite short period of loading voltage, from several dozens to hundreds of microseconds; the second one was the cantilever moved toward a certain positive direction when loading a positive voltage, and vice versa; The last one was the moving of cantilever hampered by the negative voltage when the voltage altered from positive to negative, and vice versa. Therefore, the displacement and rate of cantilevers could not arrive at the maximal value and the present linear variation rule was zero under the bias voltage.



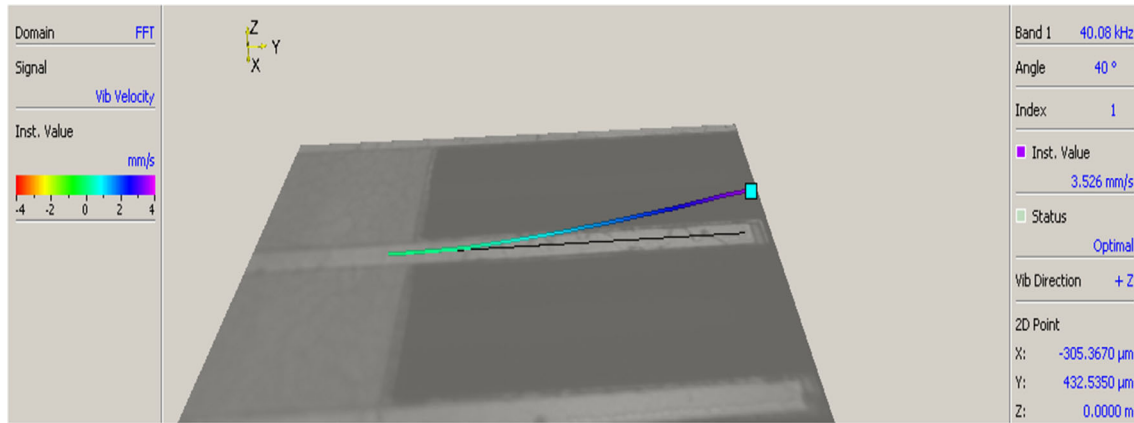


**Fig. 7** First-order vibrational model at the first response of the cantilevers

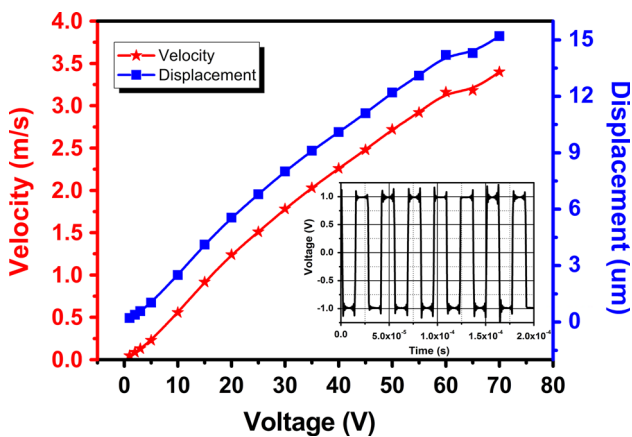


**Fig. 8**  $V(\text{velocity})/D(\text{displacement}) - V(\text{voltage})$  of PLZT micro-cantilever ( $500 \times 40 \times 10 \mu\text{m}^3$ ) with different square voltages. The inset showed original square signal of voltage varied from  $-1$  to  $1$  V

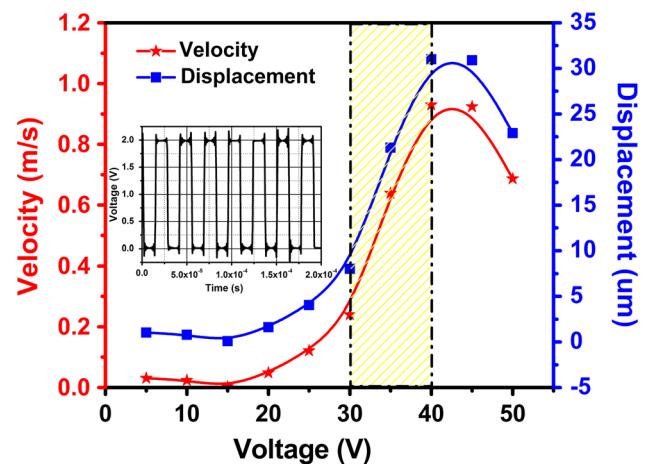


**Fig. 9**  $V(\text{velocity})/D(\text{displacement}) - V(\text{voltage})$  of PLZT micro-cantilever ( $500 \times 40 \times 10 \mu\text{m}^3$ ) with different square voltage at the first resonance frequency. The inset showed the original square signal of voltage varied from  $0$  to  $2$  V

Figure 9 showed the curve of the dependence of maximal rate and displacement variation in different square voltages of the micro-cantilevers. The square voltage signals from  $0$  to  $2$  V were applied to the AFE PLZT micro-cantilevers, shown in the inset of Fig. 9. The original voltage frequency was the natural frequency of the micro-cantilever, and the bias voltage of original voltage and amplitude of voltage were both  $1$  V. The motion law of micro-cantilever presented the switching characteristics when loading the amplified original voltage. There were three stages that could be easily recognized.

1. For the loaded voltage between  $5$  and  $30$  V, the strain had slight linearly increased due to the AFE phase mostly existing in the AFE layer of Si-based PLZT cantilevers with a quite less rate of remnant polarization. Therefore, the vibration displacement and velocity of the cantilevers increased to  $8.02 \mu\text{m}$  and  $0.24$  m/s under the voltage of  $30$  V, respectively.

2. For the loaded voltage varying from  $30$  to  $45$  V, the cantilevers showed sharp strain, and the maximal vibration displacement and maximal vibration velocity reached  $31 \mu\text{m}$  and  $0.93$  m/s at the voltage of  $40$  V, respectively. Because the AFE phase in AFE layer transitioned to the ferroelectric phase, great strain in the anti-ferroelectric layer produced the big stress of the cantilevers which conformed to phased change curves of the AFE to the ferroelectric phase [9]. In addition, the testing voltage ( $40$  V) was quite close to the calculated voltage ( $42$  V) mentioned before.
3. For the loaded voltage changing from  $45$  to  $50$  V, it showed the cantilever held almost the same strain because the AFE layer had been in the ferroelectric phase at this stage. A higher voltage could lead the cantilevers to breakdown, and hence all the tests were carried out no more than  $50$  V magnitudes.

As a result, the characteristics of phase transition for PLZT micro-cantilevers were provided, and both velocity and displacement arrived at maximal values when the amplitude of voltage was equal to or greater than the bias voltage.

## 4 Conclusions

This work presented the design and test of a Si-based AFE (Pb, La) (Zr, Ti)O<sub>3</sub> thick film micro-cantilevers with the purpose of MEMS device. The PLZT cantilevers driven by stable electric field ( $40 \pm 2$  V) had large displacement (31  $\mu$ m) and velocity (0.93 m/s), which could be suitable for MEMS devices, especially those devices that needed larger drive powers, such as micro-pumps, micro-motors, ultrasonic motors and actuators, etc.

**Acknowledgments** The authors would like to acknowledge the support from the National Science Fund for Distinguished Young Scholars under Grant No. 51225504, the National Natural Science Foundation of China under Grant Nos. 61401406, 51175483 and 51422510, Program for New Century Excellent Talents in University of China (NCET), supported by the National Science Fund for Distinguished Young Scholars under Grant No. 51225504 and Functional Materials Research Laboratory, Tongji University, China.

## References

- X.J. Chou, W.P. Geng, Y.B. Lv et al., Direct current electric field adjustable phase transformation behavior in (Pb, La) (Zr, Ti)O<sub>3</sub> antiferroelectric thick films. *J. Mater. Sci. Mater. Electron.* **24**, 861–865 (2013)
- S. Christopher. Electro-mechanical coupling in 8/65/35 PLZT, in *Proceedings of the 9th IEEE International Symposium on Applications of Ferroelectrics* (1994), pp. 357–360
- A.C. Hartley, R.E. Miles, J. Corda et al., Large throw magnetic microactuator. *Mechatronics* **18**, 459–465 (2008)
- W.Y. Pan, Q.M. Zhang, A.S. Bhalla et al., Field-forced antiferroelectric to ferroelectric switching in modified lead zirconate titanate stannate ceramics. *J. Am. Ceram. Soc.* **72**, 571–578 (1989)
- W.Y. Pan, C.Q. Dam, Q.M. Zhang et al., Cross, large displacement transducers based on electric field forced phase transitions in the tetragonal (Pb<sub>0.97</sub>La<sub>0.02</sub>) (Ti, Zr, Sn)O<sub>3</sub> family of ceramics. *J. Appl. Phys.* **66**, 6014–6023 (1989)
- T. Mineta, K. Kasai, Y. Sasaki et al., Flash-evaporated TiNiCu thick film for shape memory alloy micro actuator. *Microelectron. Eng.* **86**, 1274–1277 (2009)
- J. Jnnti, A. Łoziński, S. Leppävuori, LTCC compatible PLZT thick-films for piezoelectric devices. *Sens. Actuators A* **110**, 361–364 (2004)
- A. Furuta, K. Y. Oh, K. U. Chino. Mechanical clamper using shape memory ceramics, in *Proceedings of the 7th IEEE International Symposium on Applications of Ferroelectrics* (1990), pp. 528–529
- H.J. Zhao, Preparation and properties of PLZT thick films on silicon. *Mater. Sci. Eng. B* **99**, 195–198 (2003)
- X.J. Chou, M.X. Guo, Y.T. Zhang, Preparation and dielectric properties of highly preferred-(100) orientation (Pb, La) (Zr, Ti)O<sub>3</sub> anti-ferroelectric thick films by sol-gel processing. *Sol Gel Sci. Technol.* **61**, 62–68 (2012)
- X.J. Chou, M.X. Du, Y.B. Lv, Phase transition characterization dependent on temperature and DC electric field for (Pb, La) (Zr, Ti)O<sub>3</sub> anti-ferroelectric thick films. *Key Eng. Mater.* **503**, 97–102 (2012)
- W.P. Geng, X.J. Chou, Y.B. Lv, Structures and dielectric properties of (Pb, La) (Zr, Ti)O<sub>3</sub> anti-ferroelectric thick films prepared by different sintering procedures. *Key Eng. Mater.* **503**, 375–380 (2012)
- J. Liu, W. Geng, X.J. Chou et al., Electric field-induced phase transition characteristics at various temperatures in (Pb, La) (Zr, Ti)O<sub>3</sub> antiferroelectric thick films. *J. Sol Gel Sci. Technol.* **62**, 414–418 (2012)
- K. An, P.Q. Li, D.H. Chen et al., Phase transition current of antiferroelectric (Pb<sub>0.97</sub>La<sub>0.02</sub>) (Zr<sub>0.95</sub>Ti<sub>0.05</sub>)O<sub>3</sub> thick films under thermo-electric coupled field. *Solid State Commun.* **180**, 64–67 (2014)
- X.J. Chou, X.F. Guan, Y.B. Lv et al., Superior electrostrictive strain behavior of antiferroelectric (Pb, La) (Zr, Ti)O<sub>3</sub> thick film microcantilevers for MEMS device applications. *IEEE Electron Device Lett.* **34**, 1187–1189 (2013)
- Y.H. Yang, Z.Y. Zhao, X.F. Guan et al., Microcantilevers fabrication process of silicon-based (Pb, La) (Zr, Ti)O<sub>3</sub> antiferroelectric thick films for microactuator applications. *Appl. Mech. Mater.* **80–81**, 13–17 (2011)